frontiers in Molecular Neuroscience

ORIGINAL RESEARCH
published: 10 January 2020
doi: 10.3389/fnmol.2019.00327

# Acute Liver Failure Induces Glial Reactivity, Oxidative Stress and Impairs Brain Energy Metabolism in Rats

*Pedro Arend Guazzelli[1,2†], Giordano Fabricio Cittolin-Santos[1,2†], Leo Anderson Meira-Martins[1], Mateus Grings[1], Yasmine Nonose[1], Gabriel S. Lazzarotto[1], Daniela Nogara[2], Jussemara S. da Silva[1], Fernanda U. Fontella[1], Moacir Wajner[1,2], Guilhian Leipnitz[1], Diogo O. Souza[1,2]* and Adriano Martimbianco de Assis[1,3]*

[1]Post-graduate Program in Biological Sciences: Biochemistry, ICBS, Universidade Federal do Rio Grande do Sul—UFRGS, Porto Alegre, Brazil, [2]Department of Biochemistry, Universidade Federal do Rio Grande do Sul—UFRGS, Porto Alegre, Brazil, [3]Post-graduate Program in Health and Behavior, Health Sciences Centre, Universidade Católica de Pelotas—UCPel, Pelotas, Brazil

OPEN ACCESS

**Edited by:**
Michele Papa,
University of Campania
Luigi Vanvitelli, Italy

**Reviewed by:**
Xiaolu Zhang,
Northern Jiangsu People's Hospital (NJPH), China
Yu-Feng Wang,
Harbin Medical University, China

***Correspondence:**
Diogo O. Souza
diogo@ufrgs.br

[†]These authors have contributed equally to this work

**Received:** 12 September 2019
**Accepted:** 18 December 2019
**Published:** 10 January 2020

**Citation:**
Guazzeli PA, Cittolin-Santos GF, Meira-Martins LA, Grings M, Nonose Y, Lazzarotto GS, Nogara D, da Silva JS, Fontella FU, Wajner M, Leipnitz G, Souza DO and de Assis AM (2020) Acute Liver Failure Induces Glial Reactivity, Oxidative Stress and Impairs Brain Energy Metabolism in Rats. Front. Mol. Neurosci. 12:327. doi: 10.3389/fnmol.2019.00327

Acute liver failure (ALF) implies a severe and rapid liver dysfunction that leads to impaired liver metabolism and hepatic encephalopathy (HE). Recent studies have suggested that several brain alterations such as astrocytic dysfunction and energy metabolism impairment may synergistically interact, playing a role in the development of HE. The purpose of the present study is to investigate early alterations in redox status, energy metabolism and astrocytic reactivity of rats submitted to ALF. Adult male Wistar rats were submitted either to subtotal hepatectomy (92% of liver mass) or sham operation to induce ALF. Twenty-four hours after the surgery, animals with ALF presented higher plasmatic levels of ammonia, lactate, ALT and AST and lower levels of glucose than the animals in the sham group. Animals with ALF presented several astrocytic morphological alterations indicating astrocytic reactivity. The ALF group also presented higher mitochondrial oxygen consumption, higher enzymatic activity and higher ATP levels in the brain (frontoparietal cortex). Moreover, ALF induced an increase in glutamate oxidation concomitant with a decrease in glucose and lactate oxidation. The increase in brain energy metabolism caused by astrocytic reactivity resulted in augmented levels of reactive oxygen species (ROS) and Poly [ADP-ribose] polymerase 1 (PARP1) and a decreased activity of the enzymes superoxide dismutase and glutathione peroxidase (GSH-Px). These findings suggest that in the early stages of ALF the brain presents a hypermetabolic state, oxidative stress and astrocytic reactivity, which could be in part sustained by an increase in mitochondrial oxidation of glutamate.

**Keywords: acute liver failure, brain energy metabolism, hepatic encephalopathy, redox homeostasis, mitochondria, glial reactivity**

## INTRODUCTION

Acute liver failure (ALF) is a syndrome characterized by sudden hepatic injury and dysfunction in patients with a previously healthy liver and is associated with high lethality and morbidity (Craig et al., 2010; Bernal, 2017). The characteristic features of this condition are impaired liver synthetic function (expressed as coagulopathy), hepatic encephalopathy (HE) and, in severe cases, multi-organ failure (Craig et al., 2010; Scott et al., 2013). The manifestation of the neurological impairment under ALF varies from minor confusion, disorientation and sleep disorders to severe agitation, delirium and, in most advanced stages, coma and death (Blei and Larsen, 1999; Bernal, 2017). Indeed, the final stages of HE reach 20–25% of lethality due to cerebral edema and high intracranial pressure (Larsen and Wendon, 2008; Stravitz and Larsen, 2009) which demands rapid and aggressive treatment strategies such as liver transplantation (Acharya and Bajaj, 2018; Rajaram and Subramanian, 2018).

The molecular basis involved in the development of HE is complex and still a matter of debate and controversy. Nonetheless, ammonia appears to be the main factor in the progress of this syndrome (Bjerring et al., 2009; Hadjihambi et al., 2018). Ammonia is mostly metabolized in the liver *via* the urea cycle, and thus, ammonia bloodstream levels increase in the context of liver insufficiency (Bjerring et al., 2009; Scott et al., 2013). Ammonia can cross the blood-brain barrier by diffusion (Cooper et al., 1985) and numerous studies have shown a positive correlation between its arterial concentration and intracranial hypertension in humans (Clemmesen et al., 1999; Bernal et al., 2007).

Astrocytes occupy around one-third of the cerebral cortex volume and are involved in various neurochemical and cellular regulatory processes (Souza et al., 2019), including AFL (Scott et al., 2013). Astrocytes are the only brain cells that contain glutamine synthetase (GS), an essential enzyme of the glutamatergic system. Therefore, when ammonia concentration increases in the brain, these glial cells start to detoxify it by converting glutamate to glutamine catalyzed by GS (Martinez-Hernandez et al., 1977). Albrecht and Norenberg (2006) proposed the "Trojan Horse" hypothesis which suggests that glutamine works as a carrier of ammonia into the astrocytes' mitochondria once it is metabolized back to glutamate and ammonium, leading to oxidative stress and cell dysfunction (Albrecht and Norenberg, 2006).

Previous studies demonstrated that cultured astrocytes treated with ammonia increased reactive oxygen species (ROS) levels, such as superoxide (Murthy et al., 2001), and the same effect was seen in a hyperammonemia rat model (Kosenko et al., 1997) and clinical studies (Montes-Cortes et al., 2019). Another study showed that ammonia increased mRNA levels of heme-oxygenase-1 (HO-1)—a typical marker of oxidative stress—in rats with HE (Warskulat et al., 2002). Furthermore, the administration of antioxidants such as vitamin E, catalase (CAT), and superoxide dismutase (Ulm et al., 2007) reduced ammonia-induced astrocyte swelling in rats (Jayakumar et al., 2006).

Oxidative stress is known to induce mitochondrial permeability transition (Crompton et al., 1987), which then causes the opening of the permeability transition pore (PTP), a non-selective channel in the inner mitochondrial membrane. The PTP leads to swelling of the mitochondrial matrix, defective adenosine triphosphate (ATP) production, and oxidative phosphorylation, increasing the formation of free radicals and creating a vicious cycle that results in cellular dysfunction (Zoratti et al., 2005). Furthermore, hyperammonemia has been reported to impair energy metabolism not only due to PTP but also directly affecting enzymes involved in energy metabolism (Heidari, 2019). In this regard, previous studies demonstrated that ammonia inhibits α-ketoglutarate dehydrogenase (α-KGDH) and isocitrate dehydrogenase activities (Walker, 2014) and decreases oxygen consumption in the brain (Alman et al., 1956; Strauss et al., 2003; Iversen et al., 2009; Dam et al., 2013). Nonetheless, studies with animal models of ALF have shown that brain ATP levels were only moderately decreased and the TCA cycle was not inhibited under acute HE (Hindfelt and Siesjö, 1971; Hindfelt et al., 1977), implying that the effects of hyperammonemia on brain energy metabolism are still a matter of debate. Considering the above stated, it is urgent to expand the knowledge regarding the mechanisms that lead to astrocyte dysfunction in acute HE in order to establish innovative therapeutic strategies.

The surgical resection of the liver is a well-established and extensively studied animal model of ALF and presents the fundamental features of this disease (Eguchi et al., 1996; Madrahimov et al., 2006; Detry et al., 2013). Indeed, subtotal hepatectomy (resection of 92% of the liver mass) is a reproducible model that induces death by intracranial hypertension and brain herniation and presents a therapeutic window for assessing new therapy strategies (Eguchi et al., 1996; Detry et al., 2013; Cittolin-Santos et al., 2019). We performed in this study subtotal hepatectomy in rats and evaluated astrocyte morphology, neurochemical parameters, redox homeostasis and brain energy metabolism. The objective of the present study is to elucidate early cerebral metabolic disturbances in acute HE.

## MATERIALS AND METHODS

### Reagents

All chemicals were purchased from Sigma-Aldrich (St. Louis, MO, USA). Glucose-D, [$^{14}$C(U)] (ARC0122H) and Lactic acid, L-[11-$^{4}$C] sodium salt were purchased from American Radiolabeled Chemicals, Inc. (St. Louis, MO, USA). Glutamic acid, L-[$^{14}$C(U)] (#NEC290E250UC) and Optiphase "Hisafe" 3 (−437) scintillation liquid were purchased from PerkinElmer (Boston, MA, USA). Protein quantification was performed with the BCA Protein Assay kit from Thermo Fisher Scientific (#23227, Rockford, IL, USA), using bovine serum albumin (BSA) as standard.

### Animals

Experiments were performed on 90-day-old male Wistar rats obtained from the Central Animal House of the Department of Biochemistry, ICBS, at the Universidade Federal do Rio Grande do Sul, Porto Alegre, RS, Brazil. The animals were maintained in a 12:12 h light/dark cycle (lights on 07:00–19:00 h) and in

an air-conditioned constant temperature (22 ± 1°C) colony room with free access to water and standard commercial chow (SUPRA, Porto Alegre, RS, Brazil). The experimental protocol was approved by the Ethics Committee for Animal Research of the Universidade Federal do Rio Grande do Sul, Porto Alegre, Brazil, under the project number 29468, and followed the NIH Guide for the Care and Use of Laboratory Animals (NIH publication 85-23, revised 1996). All efforts were made to minimize the number of animals used and their suffering.

## Surgical Procedure

Subtotal hepatectomy was performed according to previous descriptions, with minor modifications (Kieling et al., 2012; Detry et al., 2013; Cittolin-Santos et al., 2019). Anesthesia was induced and maintained with 3% isoflurane and an oxygen flow of 0.8 L/min during the whole procedure. The animals were placed on a warmed operating table and a midline laparoscopy was performed to expose the liver. Hepatic ligaments were resected and then pedicles of the anterior lobes were ligated with a 4–0 silk thread to interrupt the blood flow to allow lobe resection. The same procedure was then performed on the right lobes. Only the omental lobes (8% of the liver mass) remained functional. The abdominal wall was sutured with 4–0 nylon thread. Sham group was submitted to the same protocol, except none of the liver lobes pedicles were ligated nor resected.

The animals received intramuscular lidocaine in the abdominal wound to reduce postoperative pain and were kept in a warmed box until full recovery from the anesthesia before being returned to their home cages. Animals had free access to 20% glucose in the drinking water during the whole experiment. Also, three glucose injections of the same glucose solution were administered (2 ml/kg, i.p.) after the surgery to avoid hypoglycemia at the time marks 0, 6 and 12 h.

## Tissue Preparation

Twenty-four hours after the surgery, the rats were euthanized by decapitation, and blood was immediately collected in heparinized tubes. The blood samples were then centrifuged at 2,500× *g* for 10 min at 20°C to yield the plasma fraction for subsequent biochemical analyses. Also, the same animals had samples of the cerebral cortex dissected and separated to evaluate the following parameters: (I) astrocytic reactivity; (II) oxygen consumption; (III) metabolic enzyme activities; (IV) substrates oxidation to $CO_2$; and (V) redox homeostasis.

## Immunohistochemistry and Astrocyte Morphological Analysis

Immunohistochemistry for glial fibrillary acidic protein (GFAP) positive astrocyte was performed to evaluate morphological parameters. After decapitation, brains were fixed by immersion for 24 h in 4% PFA diluted in phosphate buffer saline (PBS, pH 7.4), cryoprotected through immersion in sucrose solution (gradually, 15% to 30% until sinking) and frozen at −20°C. Coronal brain slices of 30 μm, approximately +2.20 mm rostrally from bregma, were obtained using a cryostat (MEV, SLEE Medical GMBH, Mainz, Germany). Brain slices were post-fixed with 4% PFA-PBS for 15 min., permeabilized in 0.1% Triton X-100 diluted in PBS (PBS-Tx), and then blocked for 1 h with 5% fetal goat serum diluted in PBS-Tx. The samples were incubated for 24 h at 4°C with polyclonal rabbit anti-GFAP (Z0334, 1:500 in PBS-Tx, Dako, Glostrup, Denmark), followed by 2 h incubation with goat anti-rabbit AlexaFluor® 555 secondary antibody (1:1,000 in PBS-Tx, Invitrogen, Carlsbad, CA, USA). Images were obtained in Leica TCS SP5 II laser-scanning confocal microscopy and acquired at 8-bit gray-scale (256 gray levels) using the Leica Application Suite Advanced Fluorescence software (Leica Microsystems, Munich, Germany). The Sholl's mask creation (virtual concentric circles and orthogonal lines) and all analyses were performed using the ImageJ software, a public domain Java Image processing program[1].

## Plasma Biochemical Parameters Evaluation

Plasma ammonia, glucose, lactate, alanine aminotransferase (ALT) and aspartate aminotransferase (AST) were measured using commercial kits (Lab test, MG, Brazil) and a SpectraMax M5 microplate reader (Molecular Devices, CA, USA; de Assis et al., 2009).

## Preparation of Mitochondrial Fractions

Twenty-four hours after the surgery, cerebral cortex mitochondria were isolated as previously described (Rosenthal et al., 1987) with slight modifications (Mirandola et al., 2008). Immediately after decapitation, the brain was rapidly removed, the cerebral cortex was dissected and placed into an ice-cold isolation buffer containing 225 mM mannitol, 75 mM sucrose, 1 mM EGTA, 0.1% (BSA; fatty acid-free) and 10 mM HEPES, pH 7.2. The tissue was cut into small pieces using surgical scissors and extensively washed to remove the blood and then homogenized with 1.5 ml of isolation buffer. The homogenate was centrifuged for 3 min at 2,000× *g*. After centrifugation, the supernatant was centrifuged again for 8 min at 12,000× *g*. The pellet was resuspended in 1 ml of isolation buffer containing 4 μl of 10% digitonin and centrifuged for 10 min at 12,000× *g*. The final pellet containing the mitochondria was gently washed and suspended in isolation buffer devoid of EGTA, at an approximate protein concentration of 8 mg/ml.

## Determination of Mitochondrial Respiratory Parameters by Oxygen Consumption

Oxygen consumption rate was measured using an OROBOROS Oxygraph-2k (Innsbruck, Austria) in a thermostatically controlled environment (37°C) and magnetically stirred in an incubation chamber (2 ml of standard reaction medium) in respiring medium containing 0.3 M sucrose, 5 mM KH2PO4, 1 mM EGTA, 1 mg/ml BSA, 5 mM 3-[N-morpholino] propane sulfonic acid (MOPS), pH 7.4, using glutamate plus malate (2.5 mM each) as substrates. State 3 respiration was measured

[1] http://rsb.info.nih.gov/ij/

after the addition of 1 mM ADP to the incubation medium. To measure resting (state 4) respiration, 1 μg/ml oligomycin A was added to the incubation medium. The respiratory control ratio (RCR: state 3/state 4) was then calculated. The uncoupled respiration was induced by the addition of carbonyl cyanide m-chlorophenyl hydrazone (CCCP, 2 μM). States 3, 4 and uncoupled respiration were calculated as nmol $O_2$ consumed/min/mg protein, and the results were expressed as a percentage of control.

## Determination of ATP Concentration

In order to measure brain ATP levels in frontoparietal cortex, animals were euthanized by decapitation and the whole head was immediately submerged in liquid nitrogen. Once the head was utterly frozen, brain tissue was quickly harvested with a hammer and chisel through a median craniectomy, and the brain tissue (while still frozen) was submerged in 200 μl of 0.7 N perchloric acid at 4°C. The samples were then homogenized and centrifuged (16,000× *g* for 10 min at 4°C). The supernatants were neutralized with 4.0 N KOH and clarified with second centrifugation (16,000× *g* for 30 min. at 4°C). After the second centrifugation, the supernatants were collected and centrifuged a third time (16,000× *g* for 30 min. at 4°C). ATP analysis was performed by HPLC, as previously described (Voelter et al., 1980). Aliquots of 20 μl were applied to a reversed-phase HPLC (Shimadzu, Japan) using a C18 column (Ultra C18, 25 cm × 4.6 mm × 5 μm, Restek Corporation, Bellefonte, PA, USA). The elution was carried out by applying a linear gradient from 100% solvent A (60 mM KH2PO4 and 5 mM of tetrabutylammonium chloride, pH 6.0) to 100% of solvent B (solvent A plus 30% methanol) over a 30-min period (flow rate at 1.4 ml/min). The amounts of purines were measured by absorption at 254 nm. The retention times of standards were used as parameters for identification and quantification.

## Determination of Glutamate Dehydrogenase (GDH) Activity

Glutamate dehydrogenase (GDH) activity was assayed according to Colon et al. (1986). The reaction mixture contained mitochondrial preparations (60 μg of protein), 50 mM triethanolamine buffer, pH 7.8, 2.6 mM EDTA, 105 mM ammonium acetate, 0.2 mM NADH, 10 mM α-ketoglutarate and 1.0 mM ADP. The reduction of NADH absorbance was monitored spectrophotometrically at 340 nm. GDH activity was calculated as nmol NADH/min/mg protein.

## Determination of Malate Dehydrogenase (MDH) Activity

Malate dehydrogenase (MDH) activity was measured according to Kitto et al. (1970). The incubation medium consisted of mitochondrial preparations (1 μg of protein), 10 μM rotenone, 0.1% Triton X-100, 0.14 mM NADH, 0.3 mM oxaloacetate and 50 mM potassium phosphate, pH 7.4. MDH activity was determined following the reduction of NADH fluorescence at wavelengths of excitation and emission of 366 and 450 nm, respectively. MDH activity was calculated as nmol NADH/min/mg protein.

## Determination of α-Ketoglutarate Dehydrogenase (α-KGDH) Complex Activity

The α-KGDH complex activity was evaluated according to Lai and Cooper (1986) and Tretter and Adam-Vizi (2004) with some modifications. The incubation medium contained mitochondrial preparations (250 μg of protein), 1 mM $MgCl_2$, 0.2 mM thiamine pyrophosphate, 0.4 mM ADP, 10 μM rotenone, 0.2 mM EGTA, 0.12 mM coenzyme A-SH, 1 mM α-ketoglutarate, 2 mM $NAD^+$, 0.1% Triton X-100 and 50 mM potassium phosphate, pH 7.4. The reduction of $NAD^+$ was recorded at wavelengths of excitation and emission of 366 and 450 nm, respectively. The α-KGDH activity was calculated as nmol NADH/min/mg protein.

## Determination of Citrate Synthase (Kaplan et al., 2015) Activity

CS activity was measured according to Shepherd and Garland (1969), by determining 5,5-dithio-bis (2-nitrobenzoic acid; DTNB) reduction at λ = 412 nm. The incubation medium contained mitochondrial preparations (2 μg of protein), 5 mM potassium phosphate buffer, pH 7.4, 300 mM sucrose, 1 mM EGTA, 0.1% BSA, 5 mM MOPS, 0.1% Triton X-100, 0.1 mM DTNB, 0.1 mM acetyl-CoA and 0.2 mM oxaloacetate. CS activity was calculated as nmol TNB/min/mg protein.

## Determination of Succinate Dehydrogenase (SDH) Activity

Succinate dehydrogenase (SDH) activity was measured according to Fischer et al. (1985) by determining 2,6-dichloroindophenol (DCIP) reduction at λ = 600 nm. The incubation medium contained tissue supernatant (30 μg of protein), 40 mM potassium phosphate buffer pH 7.4, 16 mM sodium succinate, 4 mM sodium azide, 7 μM rotenone, 8 μM DCIP and 1 mM phenazine methosulfate. SDH activity was calculated as nmol reduced DCIP/min/mg protein.

## Redox Assays

### Reactive Oxygen Species (ROS) Levels

To assess ROS levels, DCFH-DA was used as a probe (LeBel et al., 1992). An aliquot of the parietal cortex homogenate (100 μg–30 μl) was incubated with DCFH-DA (100 μM) at 37°C for 30 min. The formation of fluorescent DCF was monitored at excitation and emission wavelengths of 488 and 525 nm, respectively, using a fluorescence spectrophotometer. ROS contents were quantified using a DCF standard curve. The results are expressed as nmol DCF formed/mg protein.

### Antioxidant Enzymes Activities

Superoxide dismutase (Ulm et al., 2007; EC 1.15.1.1) activity was assessed on parietal cortex samples by quantifying the inhibition of superoxide-dependent adrenaline auto-oxidation at 480 nm, as previously described, and the results were expressed as units SOD/mg protein (Boveris, 1984). Glutathione peroxidase (GSH-Px; EC 1.11.1.9) activity was measured according to Wendel (1981). One unit of GSH-Px activity was defined as 1 μmol NADPH consumed/min and the specific activity is expressed as units/mg protein.

## Substrates Oxidation to $^{14}CO_2$

Cerebral cortex slices (300 μm, 100–120 mg) were obtained as described above, transferred into flasks and pre-incubated in Dulbecco's buffer for 30 min. Before incubation with substrates, the reaction medium was gassed with a 95% $O_2$:5% $CO_2$ mixture for 30 s. Slices were incubated in 1 ml of Dulbecco's buffer containing either: (i) 5 mM D-Glucose + 0.2 μCi D-[$^{14}$C(U)]glucose (American Radiolabeled Chemicals, Inc., St. Louis, MO, USA); (ii) 10 μM L-glutamic Acid + 0.2 μCi L-[$^{14}$C(U)] Glutamate (PerkinElmer Boston, MA, USA); and (iii) 10 μM sodium L-lactate + 0.2 μCi L-[U-$^{14}$C]lactate (American Radiolabeled Chemicals, Inc., St. Louis, MO, USA). Then, flasks containing the slices were sealed with rubber caps and parafilm and incubated at 37°C for 1 h in a Dubnoff metabolic shaker (60 cycles/min) as described previously (Dunlop et al., 1975; Ferreira et al., 2007). The incubation was stopped by adding 0.2 ml of 50% trichloroacetic acid (TCA) through the rubber cap into the flask while 0.1 ml of 2 N NaOH was injected into the central wells. Thereafter, flasks were shaken for an additional 30 min. at 37°C to trap $CO_2$. Afterward, the content of the central well was transferred to vials and assayed for $^{14}CO_2$ radioactivity in a liquid scintillation counter. All the results are expressed as nmol of substrate oxidized per mg of tissue and the initial specific activity of the incubation medium was considered for calculations (Müller et al., 2013).

## Statistical Analysis

The data are expressed as mean ± SEM. All analyses were performed with Prism GraphPad (Version 6.01 for Windows, GraphPad Software, San Diego, CA, USA[2]). Differences among the groups were analyzed by *t*-test with levels of significance below $p < 0.05$ indicated in the following section.

# RESULTS

An initial cohort of 20 animals was operated on and observed to evaluate the efficiency of the surgical procedure and compare it to previous reports (Cittolin-Santos et al., 2019). Our findings were similar to previous studies demonstrating 80% lethality from 30 to 60 h after the surgical procedure (**Supplementary Figure S1**; Cittolin-Santos et al., 2019). Considering the above stated, a 24-h post-surgery time mark was chosen to collect blood and brain samples, because at this point all animals presented signs of encephalopathy although most were still alive. The second cohort of animals was operated on to obtain samples of blood or cerebral cortex (frontoparietal), and the third cohort of animals were later operated on to perform brain ATP measurement.

## Plasma Biochemical Parameters

In **Table 1**, we observed that the hepatectomy group presented several plasma alterations that are consistent with ALF, as previously described (Eguchi et al., 1996; Detry et al., 2013; Cittolin-Santos et al., 2019). Hepatectomized animals presented higher levels of ammonia (HEPATEC: 48.4 ± 3.9 vs. SHAM: 22.4 ± 2.1; μmol/L, $p < 0.001$), lactate (HEPATEC: 5.2 ± 1.1 vs. SHAM: 1.5 ± 0.4; mg/dL, $p < 0.001$), ALT (HEPATEC: 61.6 ± 3.1 vs. SHAM: 38.1 ± 1.8 U/L, $p < 0.001$) and AST (HEPATEC: 54.9 ± 4.5 vs. SHAM: 32.6 ± 2.7 U/L, $p < 0.001$) than the controls. The hepatectomy group presented lower levels of glucose (HEPATEC: 71 ± 9 vs. SHAM: 99 ± 8; mg/dL, $p < 0.05$) compared to the sham group.

**TABLE 1** | Plasma biochemical parameters.

| | Sham | Hepatectomy |
|---|---|---|
| Ammonia (μmol/L) | 22.4 ± 2.1 | 48.4 ± 3.9*** |
| Glucose (mg/dL) | 99 ± 8 | 71 ± 9* |
| Lactate (mg/dL) | 1.5 ± 0.4 | 5.2 ± 1.1*** |
| ALT (U/L) | 38.1 ± 1.8 | 61.6 ± 3.1*** |
| AST (U/L) | 32.6 ± 2.7 | 54.9 ± 4.5*** |

*Twenty-four hours after hepatectomy, animals with acute liver failure (ALF) presented higher levels of ammonia (48.4 ± 3.9 vs. 22.4 ± 2.1; μmol/L), lactate (5.2 ± 1.1 vs. 1.5 ± 0.4; mg/dL), ALT (61.6 ± 3.1 vs. 38.1 ± 1.8 U/L) and AST (54.9 ± 4.5 vs. 32.6 ± 2.7 U/L) than the controls. The hepatectomy group presented lower levels of glucose (71 ± 9 vs. 99 ± 8; mg/dL) compared to the sham-operated group. *$p < 0.05$ and ***$p < 0.001$ indicate a significant difference from the sham-operated group (t-test).*

## Immunohistochemistry and Astrocyte Morphological Analysis

Confocal images of parietal cortex stained with GFAP showed that animals with ALF (**Figure 1A**) presented an increase in the number of astrocytes/mm$^3$ (HEPATEC: 3.05 ± 0.20 vs. SHAM: 2.44 ± 0.16, **Figure 1B**, $p < 0.05$) as well as in regional optical density (HEPATEC: 4.99 ± 1.12 vs. SHAM: 3.41 ± 1.16, **Figures 1C,D**, $p < 0.05$) and in cellular optical density (HEPATEC: 87.60 ± 7.39 vs. SHAM: 57.22 ± 15.21, **Figure 1E**, $p < 0.001$) when compared to the control animals. The area and the volume occupied by astrocytes was also increased when compared to the sham group (HEPATEC: 36.57 ± 2.42 vs. SHAM: 29.24 ± 1.90 and HEPATEC: 24.38 ± 1.61 vs. SHAM: 19.49 ± 1.27, respectively, **Figures 1F,G**, $p < 0.05$). Nonetheless, the number of brain cells was equal in both groups (data not shown). Regarding cellular morphology (**Figure 2A**), the astrocytes of hepatectomized animals presented a general increase in the ratio of Central processes/lateral processes (LP; HEPATEC: 0.82 ± 0.03 vs. SHAM: 1.09 ± 0.04, **Figure 2B**, $p < 0.05$), number of primary processes (HEPATEC: 3.74 ± 0.23 vs. SHAM: 2.97 ± 0.21, **Figure 2C**, $p < 0.05$) and secondary processes (HEPATEC: 1.46 ± 0.43 vs. SHAM: 0.46 ± 0.26, **Figure 2D**, $p < 0.001$). Consequentially, the number of intersections between these cellular processes was also significantly increased in animals with ALF when compared to the sham group (HEPATEC: 24.74 ± 2.13 vs. SHAM: 13.85 ± 5.62, **Figure 2E**, $p < 0.01$). Additional analysis of astrocytic morphology is also expressed in **Supplementary Figure S2** .

## Oxygen Consumption

Mitochondrial oxygen consumption was mostly increased in animals with HE compared to the control group. Indeed, an elevated oxygen consumption level was found in state 3 (HEPATEC: 118.20 ± 9.58 vs. SHAM: 100.00 ± 7.90, **Figure 3A**, $p < 0.01$), in-state 4 (HEPATEC: 112.80 ± 8.63 vs. SHAM: 100.00 ± 9.73 m, **Figure 3B**, $p < 0.05$) and in uncoupled respiration (CCCP; HEPATEC: 116.40 ± 13.09 vs. SHAM: 100.00 ± 10.31,

[2]www.graphpad.com

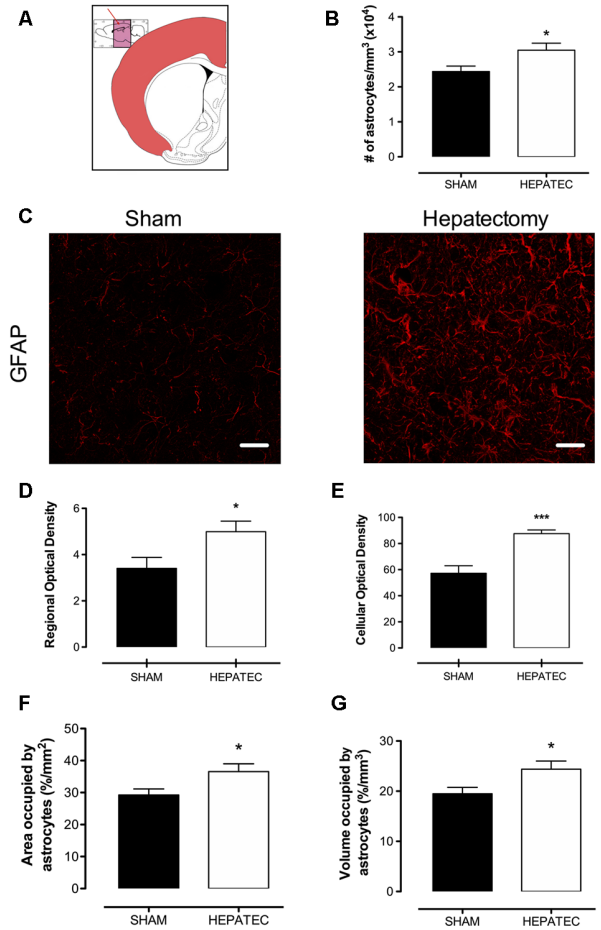


**FIGURE 1** | Immunofluorescence for glial fibrillary acidic protein (GFAP). Panel **(A)** represents the region of the brain that was analyzed—parietal cortex; panel **(B)** represents the number of astrocytes/mm$^3$; panel **(C)** represents immunofluorescence for the GFAP in the parietal cortex. The hepatectomy group presented an increase in regional immunofluorescence for GFAP **(D)** and cellular optical density (87.60 ± 7.39 vs. 57.22 ± 15.21) **(E)**. The area occupied by astrocytes (36.57 ± 2.42 vs. 29.24 ± 1.90) **(F)** and the volume occupied by astrocytes (24.38 ± 1.61 vs. 19.49 ± 1.27) **(G)** were also augmented. Differences between groups were analyzed by *t*-test and are indicated as $*p < 0.05$ and $***p < 0.001$.

**Figure 3C**, $p < 0.05$). No alterations were found in the RCR (HEPATEC: 102.10 ± 7.47 vs. SHAM: 100.00 ± 7.15, **Figure 3D**). Results are expressed as a percentage of control.

## ATP Levels

Parietal cortex ATP levels were significantly elevated in animals with ALF (HEPATEC: 1.20 ± 0.13 vs. SHAM: 0.63 ± 0.05, **Figure 3E**, $p < 0.05$), as expressed in **Figure 3E**. Results are expressed as μmol/mg of tissue.

## Enzyme Activities of Brain Energy Metabolism

Hepatectomized animals presented increased activity in all evaluated metabolic enzymes when compared to the sham group (**Figure 4**). Enzyme activity in hepatectomized and control group was, respectively: citrate synthase (HEPATEC: 201.05 ± 16.11 vs. SHAM: 171.10 ± 20.03, **Figure 4A**, $p < 0.05$); MDH (HEPATEC: 133,954 ± 8,690 vs. SHAM: 98,149 ± 30,939, **Figure 4B**, $p < 0.05$); SDH (HEPATEC: 12.22 ± 1.46 vs. SHAM: 10.65 ± 0.39, **Figure 4C**, $p < 0.05$); α-KGDH (HEPATEC: 7.29 ± 0.59 vs. SHAM: 5.85 ± 0.71, **Figure 4D**, $p < 0.05$); and GDH (HEPATEC: 339.1 ± 8.24 vs. SHAM: 299.90 ± 46.46, **Figure 4E**, $p < 0.01$). The results are expressed as nmol of substrate/min/mg of protein.

## Substrates Oxidation to $^{14}CO_2$

Animals submitted to hepatectomy presented an increase in glutamate oxidation to $^{14}CO_2$ (HEPATEC: 9.36 ± 0.82 vs. SHAM: 6.11 ± 0.45, **Figure 5A**, $p < 0.01$) while presenting lower oxidation to $^{14}CO_2$ of glucose (HEPATEC: 511.30 ± 38.86 vs. SHAM: 591.80 ± 80.97, **Figure 5B**, $p < 0.05$) and lactate (HEPATEC: 2,602.0 ± 228.90 vs. SHAM: 3,142.0 ± 266.50, **Figure 5C**, $p < 0.05$). The results are expressed as pmol of substrate/min/mg of tissue.

## Redox Assays

Several alterations in the redox homeostasis were induced by hepatectomy. Acute HE presented elevated levels of ROS (HEPATEC: 757.80 ± 36.82 vs. SHAM: 417.00 ± 22.54, **Figure 6A**, $p < 0.001$). Accordingly, it caused a decrease in the activity of two essential antioxidant enzymes: SOD (HEPATEC: 26.62 ± 1.19 vs. SHAM: 33.54 ± 1.38, **Figure 6B**, $p < 0.001$) and GSH-Px (HEPATEC: 21.90 ± 1.32 vs. SHAM: 27.55 ± 1.89, **Figure 6C**, $p < 0.05$). PARP-1 immunocontent in the cerebral cortex of hepatectomized animals was elevated when compared to the sham group (HEPATEC: 0.089 ± 0.002 vs. SHAM: 0.078 ± 0.001, respectively, **Figure 6D**, $p < 0.01$).

# DISCUSSION

ALF is a meaningful and potentially life-threatening syndrome that is caused by liver damage and substantial neurotoxin accumulation in the brain, such as ammonia (Bernal, 2017). Indeed, blood ammonia elevation plays an essential role in the development of encephalopathy and leads to glutamatergic excitotoxicity, oxidative stress and astrocytic dysfunction (Cieńko-Michalska et al., 2012; Butterworth, 2015). In the present study, we used an experimental model of ALF induced by subtotal hepatectomy to investigate astrocyte reactivity, brain redox status, energy metabolism and mitochondrial function in rodents. To our knowledge, this is the first study describing evidence of a brain hypermetabolic state induced by ALF, as previous similar results had been found only using cell cultures or acute ammonium intoxication models (Kosenko et al., 1994; Xue et al., 2010). The hypermetabolic state involved the increase in brain oxygen consumption and activities of mitochondrial enzymes, elevated ATP levels, and increased glutamate oxidation. We also postulate a new link between the hypermetabolic state of HE and the increase of ROS with astrocytic reactivity, suggesting a new understanding of the early (24 h) brain metabolic profile in acute HE.

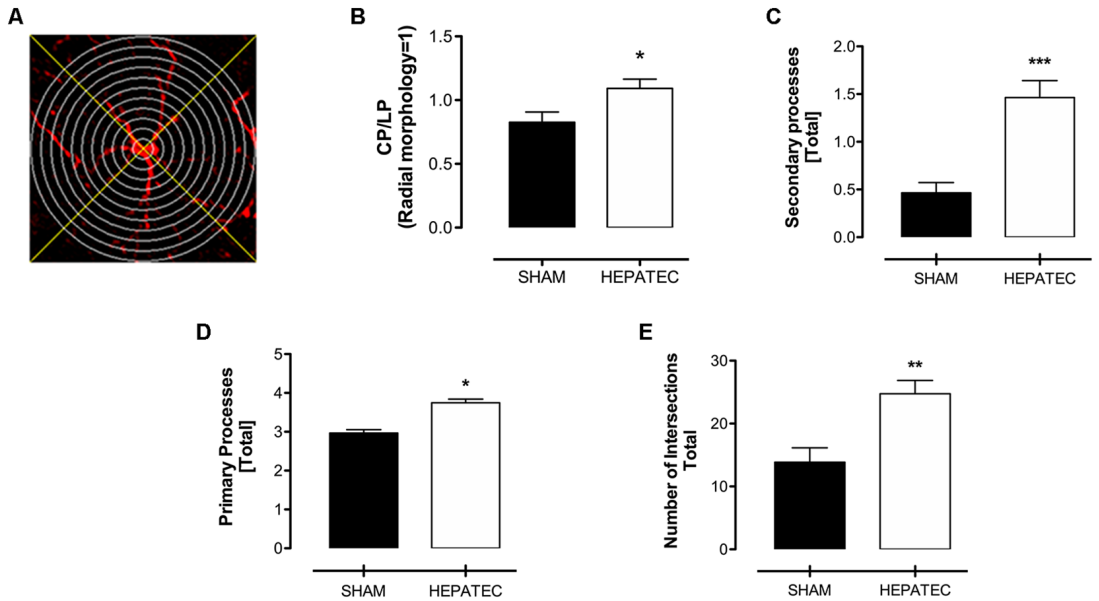


**FIGURE 2 |** Sholl's mask creation—virtual concentric circles and orthogonal lines **(A)** and astrocytic processes and intersections. Panel **(B)** expresses the ratio between central processes (McPhail et al., 2010) and lateral processes (LP; 1.09 ± 0.07 vs. 0.83 ± 0.08). Hepatectomy group presented an increase in the size of both cellular primary processes **(C)** (19.68 ± 1.41 vs. 12.90 ± 1.31) and secondary processes **(D)** (1.46 ± 0.43 vs. 0.46 ± 0.26). The number of intersections **(E)** was also increased in animals operated on (24.74 ± 2.13 vs. 13.85 ± 5.62). Differences between groups were analyzed by *t*-test and are indicated as $^{*}p < 0.05$; $^{**}p < 0.01$ and $^{***}p < 0.001$.

For this discussion, it is crucial to emphasize that hepatectomy causes up to 80% lethality in the interval from 30 to 60 h after surgery (**Supplementary Figure S1**), as demonstrated in the previous work of our group (Cittolin-Santos et al., 2019). Therefore, the 24-h time mark after surgery was chosen to harvest blood and brain samples as most animals were still alive and already showing marked signs of HE such as ataxia, lethargy and diminished response to pain (Cauli et al., 2008). At this point, animals also presented elevated plasma liver enzymes and alterations in blood glucose, lactate and ammonia levels (**Table 1**) that are well described in this animal model of ALF (Eguchi et al., 1996; Detry et al., 2013; Fusco et al., 2013; Cittolin-Santos et al., 2019).

As mentioned before, elevated intracranial pressure is an essential contributor to HE's high lethality rates (Larsen and Wendon, 2008) and understanding the mechanisms that contribute to this process may be vital in establishing better patient care. Previous studies with magnetic resonance imaging performed in humans with ALF have shown a reduction in the brain's apparent diffusion coefficient, indicating an increase in cellular volume and brain edema (Keiding and Pavese, 2013). Indeed, ALF induces an accumulation of glutamine in the astrocyte in an attempt to detoxify ammonia which has been linked to astrocyte swelling and dysfunction due to glutamine's osmolyte effect (Scott et al., 2013; Rama Rao et al., 2014). In parallel, astrocytic reactivity may be a defense mechanism to modulate brain homeostasis by increasing astrocytic workload, and it may contribute to the elevation of brain pressure due to increased cellular volume. This process has been described in several cerebral diseases, including experimental and human HE (Pilbeam et al., 1983; Kimura et al., 2008). In this manuscript, we describe severe astrocytic morphological changes that characterize a state of diffuse astrocytic reactivity. Indeed, we encountered a significant increase in cellular optical density and astrocytic volume consequential to the increase of astrocytic processes. No alterations were found in the number of astrocytes, indicating that the increase in GFAP density was due to the proliferation in size and number of astrocytic processes. Previous work using the same ALF experimental model that our study used demonstrated an increase in the intracranial pressure following hepatectomy in rats (Detry et al., 2013). Although we did not directly measure intracranial pressure, we demonstrate a state of diffuse astrocytic growth early in the development of HE which could indicate that cytotoxic edema may not be the only mechanism involved in the expansion of the total astrocytic volume and resulting increased intracranial pressure.

Regarding mitochondrial function and brain bioenergetics, there are controversial data about the influence of hyperammonemia on TCA enzymatic activity and energy production (Schousboe et al., 2014; Heidari, 2019). Classic *in vitro* studies has shown that ammonium intoxication inhibits critical enzymes in brain energy metabolism (Bessman and Bessman, 1955). On the other hand, excess ammonium leads to a disturbance in glutamatergic homeostasis which has been linked to increased glycolysis (increased activity of phosphofructokinase and aldolase) and increased activity of TCA enzymes (Zwingmann et al., 2003). Normal brain ATP levels and TCA activity have been described in hyperammonemia

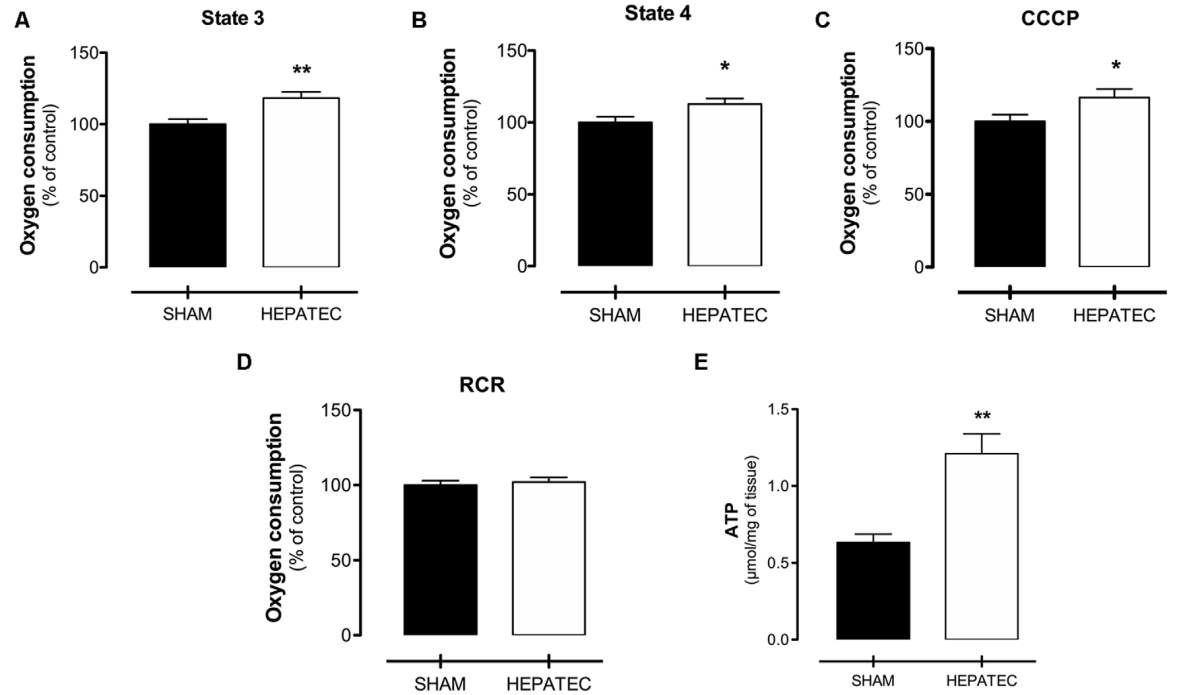


**FIGURE 3 |** Mitochondrial oxygen consumption. Animals with acute liver failure (ALF) presented higher oxygen consumption in mitochondrial state 3 (118.20 ± 9.58 vs. 100.00 ± 7.90 as % of control and 833.91 ± 93.51 vs. 753.91 ± 79.42 as pmol/s/mg) **(A)**; mitochondrial state 4 (112.80 ± 8.63 vs. 100.00 ± 9.73 as % of control and 121.26 ± 14.68 vs. 111.83 ± 10.88 as pmol/s/mg) **(B)** and CCCP (116.40 ± 13.09 vs. 100.00 ± 10.31 as % of control and 858.81 ± 115.82 vs. 792.22 ± 99.09 as pmol/s/mg) **(C)**. No differences were found in respiratory control ratio (RCR) oxygen consumption (102.10 ± 7.47 vs. 100.00 ± 7.15 as % of control and 6.90 ± 0.50 vs. 6.76 ± 0.48 as pmol/s/mg) **(D)**. Brain ATP was also augmented in animals with ALF [1.20 ± 0.13 vs. 0.63 ± 0.05, **(E)**, $p < 0.05$, µmol/mg]. **(E)** The results in the figure are expressed as (% of control). Differences between groups were analyzed by *t*-test and are indicated as $^{*}p < 0.05$ and $^{**}p < 0.01$.

and soon after experimental liver devascularization (Holmin et al., 1983; Fitzpatrick et al., 1989; Mans et al., 1994). In our current study, we found that the enzymatic activity of pathways involved in bioenergetics metabolism and oxygen consumption were elevated 24 h after hepatectomy, which was accompanied by elevated brain cortical ATP levels and thus indicating a significant alteration in the energy metabolism homeostasis. Since the alterations in brain bioenergetics follow the rapid rise in ammonium levels due to liver insufficiency, we hypothesize that the astrocytes require high levels of energy consumption to remove glutamate from the synaptic cleft and metabolize it in the TCA cycle. Thus, the increase in oxygen consumption and enzymatic activity could be a reactive mechanism of the neural cells trying to provide enough energy to enable the neural tissue to respond to brain injury, which characterizes a hypermetabolic state. This effect, however, is probably time-dependent, occurring only in the early stages (acute phase) of HE. Indeed, previous evaluations of brain ATP levels found that early HE presented mild elevations of brain ATP 4 h after total hepatectomy (Holmin et al., 1983) while ATP measurement of animals with chronic exposure to high ammonia levels (4 weeks after bile duct ligation) have demonstrated decreased ATP levels (Dhanda et al., 2018).

As stated above, astrocytes are involved in the progression of HE and some authors even propose that HE is primarily a glyopathy (Norenberg, 1996; El Khiat et al., 2019) as these cells are responsible for most of the ammonium and glutamate detoxification. This process, however, consumes a significant amount of glucose to produce glutamine and absorb two ammonia molecules which can lead to a decrease in glucose oxidation to $CO_2$. Indeed, Sibson et al. (2001) demonstrated that up to 80% of brain glucose is utilized for ammonia detoxification by glutamine formation in rats with hyperammonemia, while healthy animals utilize around 30% of glucose in this process (Sibson et al., 2001). In our study, both glucose and lactate oxidation to $CO_2$ decreased in animals with HE (**Figure 5**). Nonetheless, several reports of experimental models with acute rises in ammonia levels failed to demonstrate a brain energy deficit (Lin and Raabe, 1985; Fitzpatrick et al., 1989; Mans et al., 1994), and our data indicate elevated mitochondrial oxygen consumption as well as no ATP deficit. This could mean that some compensatory mechanisms are activated during hyperammonemia to sustain energy balance. Johansen et al. (2007) discuss the role of branched-chain amino acids in the reposition of carbon skeletons and glutamate production under HE. In this study, we found that the oxidation of glutamate to $CO_2$ was significantly increased in animals 24 h after hepatectomy (**Figure 5**). We propose that the increase in ammonia levels due to ALF augments the utilization of glucose for glutamine production contributing to the decrease of glucose

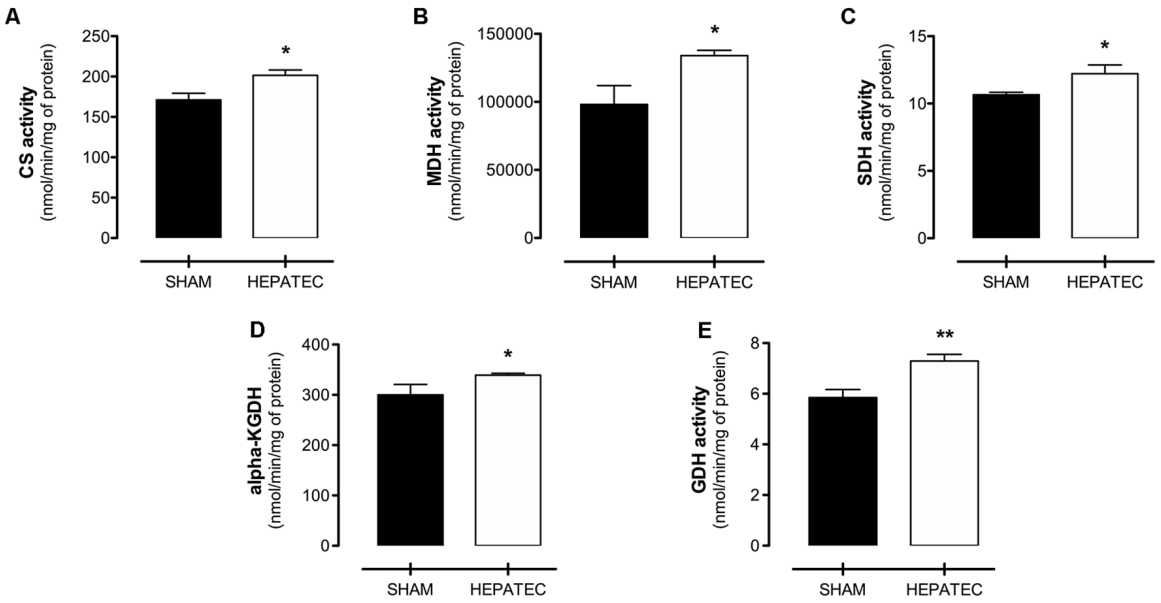


**FIGURE 4 |** Enzyme activities of brain energy metabolism. Hepatectomy group was found to have an increase in the activity of all analyzed enzymes: **(A)** Citrate synthase (201.05 ± 16.11 vs. 171.10 ± 20.03); **(B)** Malate dehydrogenase (MDH; 133,954 ± 8,690 vs. 98,149 ± 30,939); **(C)** Succinate dehydrogenase (SDH; 12.22 ± 1.46 vs. 10.65 ± 0.39); **(D)** Alpha-ketoglutarate dehydrogenase (α-KGDH; 7.29 ± 0.59 vs. 5.85 ± 0.71); and **(E)** Glutamate dehydrogenase (GDH; 339.1 ± 8.24 vs. 299.90 ± 46.46). The results are expressed as nmol/min/mg of protein. Differences between groups were analyzed by *t*-test and are indicated as $^{*}p < 0.05$ and $^{**}p < 0.01$.


**FIGURE 5 |** Substrate oxidation to $CO_2$. Animals submitted to hepatectomy presented elevated glutamate oxidation (9.36 ± 0.82 vs. 6.11 ± 0.45) **(A)**. However, the hepatectomy group had lower oxidation of glucose (511.30 ± 38.86 vs. 591.80 ± 80.97) **(B)** and lactate (2,602.0 ± 228.90 vs. 3,142.0 ± 266.50) **(C)** when compared to control animals. Results are expressed in pmol/min/mg of tissue. Differences between groups were analyzed by *t*-test and are indicated as $^{*}p < 0.05$ and $^{**}p < 0.01$.

oxidation to $CO_2$. Moreover, the increased glutamate oxidation could, in part, contribute to sustaining brain energy homeostasis as well as removing excess glutamate from the synaptic cleft and potentially attenuating the glutamatergic excitotoxicity and NMDA overstimulation.

Ammonium accumulation in the central nervous system, as described in experimental models of ammonium intoxication and ALF, causes overstimulation of NMDA receptors (Montana et al., 2014; Oja et al., 2017; Dabrowska et al., 2018). This happens both by an increase in extracellular glutamate levels and by direct ammonium activation of NMDA receptors. The NMDA receptor overstimulation is a crucial factor in the development of oxidative stress (Sathyasaikumar et al., 2007; Cittolin-Santos et al., 2017) due to the increase of calcium influx into the cell, which in turn increases ROS production (Hermenegildo et al., 2000; Montes-Cortes et al., 2019). The hepatectomy group presented elevated levels of ROS and decreased activity of SOD and GSH-Px (**Figures 6B,C**). Similar results regarding SOD activity were previously described in acute ammonia intoxication in rats by our group and others (Kosenko et al., 1998; Görg et al., 2013; Cittolin-Santos et al., 2017). This means that ammonia may cause an imbalance in brain redox status through antioxidant enzymes inhibition as well as glutamatergic overstimulation. Indeed, our group and others have shown that by modulating glutamatergic

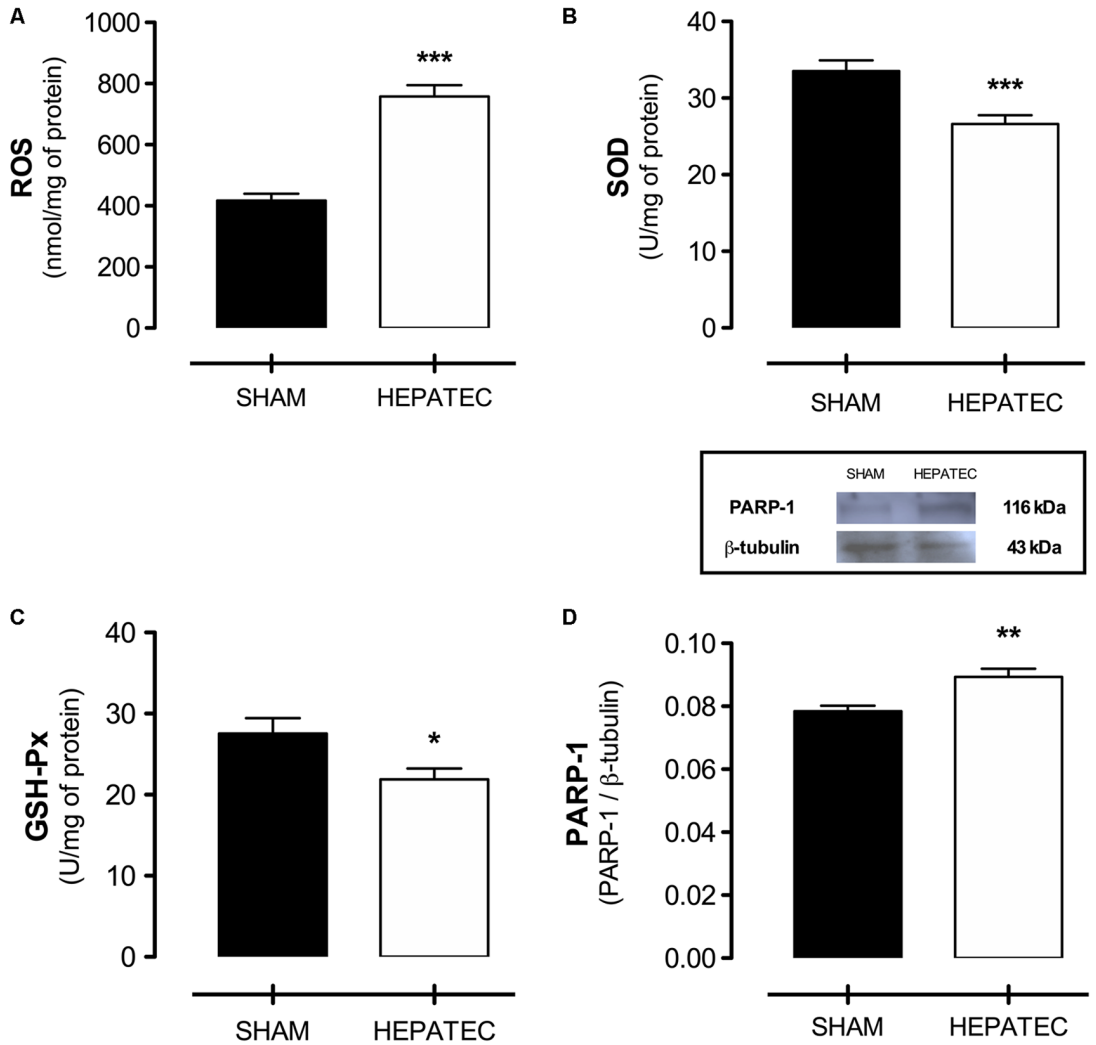


**FIGURE 6 |** Redox homeostasis and PARP-1 expression. The hepatectomy group presented elevated levels of reactive oxygen species (ROS) **(A)** (757.80 ± 36.82 vs. 417.00 ± 22.54) as well as decreased SOD **(B)** (26.62 ± 1.19 vs. 33.54 ± 1.38) and GSH-Px **(C)** (21.90 ± 1.32 vs. 27.55 ± 1.89) activity. An increased expression in PARP-1 content was also encountered in this group of animals **(D)** (0.089 ± 0.002 vs. 0.078 ± 0.001). ROS are expressed as nmol/mg of protein; the enzyme activity is expressed as U/mg of protein and PARP-1 expression as PARP-1 / b-tubulin ratio. Differences between groups were analyzed by *t*-test and are indicated as $*p < 0.05$; $**p < 0.01$ and $***p < 0.001$.

excitotoxicity there is a normalization of brain redox status and a decrease in lethality under acute ammonia intoxication (Cauli et al., 2014; Paniz et al., 2014; Cittolin-Santos et al., 2017).

Poly (ADP-ribose) polymerase 1 (PARP-1) is a nuclear enzyme involved in critical cellular processes such as DNA repair and cell death (Jubin et al., 2016). The enzymatic activity of PARP-1 is stimulated significantly in the presence of a wide range of activators like damaged DNA, nucleosomes and various protein-binding partners (Eustermann et al., 2011; Langelier et al., 2011). It is noteworthy that oxidative stress induces DNA damage in neural cells (Guo et al., 2013; Narciso et al., 2016) which may act as the signal to activate PARP-1. PARP-1 upregulation has already been linked to increased lethality in experimental models of ALF induced by acetaminophen intoxication, just as PARP-1 inhibition was related to a diminished lethality rate (Dönmez et al., 2015). Considering the above stated and the elevated levels of ROS presented in this manuscript, we hypothesize that oxidative stress is an early event in the development of acute HE that may induce DNA genic activation and PARP-1 upregulation in ALF.

Understanding the complexity of brain metabolic alterations, glial reactivity and cellular dysfunction are the first steps for the development of new treatment strategies for HE due to ALF. In this work, we described several astrocytic alterations that characterize a state of astrocytic reactivity, here observed as an increase in the astrocytic volume due to the proliferation of cellular processes that are known to take part in the pathophysiology of acute HE. We also associated these glial morphological alterations with significant brain metabolic abnormalities such as redox imbalance, increased brain energy

metabolism (increased oxygen consumption and enzymatic activities), increased brain ATP levels as well as alterations in substrate oxidation.

Furthermore, as discussed above, glutamine production for ammonia detoxification utilizes an increased amount of glucose in animals with HE. Thus, we propose that the increase in glutamate oxidation may contribute to sustaining brain ATP levels in the early stages of HE. We also found that the brain hypermetabolic state is associated with imbalances in redox homeostasis and upregulation of PARP-1. Finally, we bring new evidence to the literature regarding the association between astrocytic reactivity, oxidative stress and alterations in brain mitochondrial metabolic and in substrate oxidation under experimental ALF.

## DATA AVAILABILITY STATEMENT

All datasets generated for this study are included in the article/**Supplementary Material**.

## ETHICS STATEMENT

The animal study was reviewed and approved by Ethics Committee for Animal Research of the Universidade Federal do Rio Grande do Sul (29468), Porto Alegre, Brazil.

## AUTHOR CONTRIBUTIONS

PG and GC-S were responsible for the design, acquisition, analysis, interpretation, drafting, and approval of the final version of the manuscript. LM-M, MG, YN, GSL, DN, JS and FF were responsible for acquisition, analysis, interpretation, and approval of the final version of the manuscript. MW and GL were responsible for interpretation, drafting, critical revision, and approval of the final version of the manuscript. DS and AA were responsible for the design, interpretation, drafting, critical revision, and approval of the final version of the manuscript.

## FUNDING

This work was supported by Brazilian agencies and grants: Conselho Nacional de Desenvolvimento Científico e Tecnológico (CNPq), Coordenação de Aperfeiçoamento de Pessoal de Nível Superior (CAPES/CSF 88881.030387/2013-01), INCT—Excitotoxicity, and Neuroprotection (465671/2014-4).

## SUPPLEMENTARY MATERIAL

The Supplementary Material for this article can be found online at: https://www.frontiersin.org/articles/10.3389/fnmol.2019.00327/full#supplementary-material.

**FIGURE S1 |** Experimental protocol and subtotal hepatectomy lethality. Panel **(A)** represents the surgical protocol and time mark of 24 h post-surgery for sample harvesting. Panel **(B)** represents the overall mortality and of animals after the hepatectomy. The animals operated on presented 80% lethality within the first 30–60 h after the procedure.

**FIGURE S2 |** Astrocytic processes and intersections. The hepatectomy group presented an increase in the number of **(A)** central primary processes ($1.75 \pm 0.20$ vs. $1.23 \pm 0.08$); **(C)** central secondary processes ($0.76 \pm 0.08$ vs. $0.19 \pm 0.08$); and **(D)** lateral secondary processes ($0.70 \pm 0.14$ vs. $0.27 \pm 0.06$). The number of **(B)** lateral primary processes was equal in both groups ($1.99 \pm 0.17$ vs. $1.74 \pm 0.10$). The number of central **(E)** and lateral **(F)** intersections was also increased in animals with acute liver failure ($11.79 \pm 2.19$ vs. $5.90 \pm 0.98$ and $13.42 \pm 1.70$ vs. $7.56 \pm 1.44$, respectively). Differences between groups were analyzed by *t*-test and are indicated as $^{*}p < 0.05$; $^{**}p < 0.01$ and $^{***}p < 0.001$.

## REFERENCES

Acharya, C., and Bajaj, J. S. (2018). Current management of hepatic encephalopathy. *Am. J. Gastroenterol.* 113, 1600–1612. doi: 10.1038/s41395-018-0179-4

Albrecht, J., and Norenberg, M. D. (2006). Glutamine: a Trojan horse in ammonia neurotoxicity. *Hepatology* 44, 788–794. doi: 10.1002/hep.21357

Alman, R. W., Ehrmantraut, W. R., Fazekas, J. F., and Ticktin, H. E. (1956). Cerebral metabolism in hepatic insufficiency. *Am. J. Med.* 21, 843–849. doi: 10.1016/0002-9343(56)90098-5

Bernal, W. (2017). Acute liver failure: review and update. *Int. Anesthesiol. Clin.* 55, 92–106. doi: 10.1097/aia.0000000000000141

Bernal, W., Hall, C., Karvellas, C. J., Auzinger, G., Sizer, E., and Wendon, J. (2007). Arterial ammonia and clinical risk factors for encephalopathy and intracranial hypertension in acute liver failure. *Hepatology* 46, 1844–1852. doi: 10.1002/hep.21838

Bessman, S. P., and Bessman, A. N. (1955). The cerebral and peripheral uptake of ammonia in liver disease with an hypothesis for the mechanism of hepatic coma. *J. Clin. Invest.* 34, 622–628. doi: 10.1172/jci103111

Bjerring, P. N., Eefsen, M., Hansen, B. A., and Larsen, F. S. (2009). The brain in acute liver failure. A tortuous path from hyperammonemia to cerebral edema. *Metab. Brain Dis.* 24, 5–14. doi: 10.1007/s11011-008-9116-3

Blei, A. T., and Larsen, F. S. (1999). Pathophysiology of cerebral edema in fulminant hepatic failure. *J. Hepatol.* 31, 771–776. doi: 10.1016/s0168-8278(99)80361-4

Boveris, A. (1984). Determination of the production of superoxide radicals and hydrogen peroxide in mitochondria. *Methods Enzymol.* 105, 429–435. doi: 10.1016/s0076-6879(84)05060-6

Butterworth, R. F. (2015). Pathogenesis of hepatic encephalopathy and brain edema in acute liver failure. *J. Clin. Exp. Hepatol.* 5, S96–S103. doi: 10.1016/j.jceh.2014.02.004

Cauli, O., Gonzalez-Usano, A., Cabrera-Pastor, A., Gimenez-Garzo, C., Lopez-Larrubia, P., Ruiz-Sauri, A., et al. (2014). Blocking NMDA receptors delays death in rats with acute liver failure by dual protective mechanisms in kidney and brain. *Neuromolecular Med.* 16, 360–375. doi: 10.1007/s12017-013-8283-5

Cauli, O., Rodrigo, R., Boix, J., Piedrafita, B., Agusti, A., and Felipo, V. (2008). Acute liver failure-induced death of rats is delayed or prevented by blocking NMDA receptors in brain. *Am. J. Physiol. Gastrointest. Liver Physiol.* 295, G503–G511. doi: 10.1152/ajpgi.00076.2008

Ciećko-Michalska, I., Szczepanek, M., Slowik, A., and Mach, T. (2012). Pathogenesis of hepatic encephalopathy. *Gastroenterol. Res. Pract.* 2012:642108. doi: 10.1155/2012/642108

Cittolin-Santos, G. F., de Assis, A. M., Guazzelli, P. A., Paniz, L. G., da Silva, J. S., Calcagnotto, M. E., et al. (2017). Guanosine exerts neuroprotective effect in an experimental model of acute ammonia intoxication. *Mol. Neurobiol.* 54, 3137–3148. doi: 10.1007/s12035-016-9892-4

Cittolin-Santos, G. F., Guazzelli, P. A., Nonose, Y., Almeida, R. F., Fontella, F. U., Pasquetti, M. V., et al. (2019). Behavioral, neurochemical and brain oscillation abnormalities in an experimental model of acute liver failure. *Neuroscience* 401, 117–129. doi: 10.1016/j.neuroscience.2018.12.032

Clemmesen, J. O., Larsen, F. S., Kondrup, J., Hansen, B. A., and Ott, P. (1999). Cerebral herniation in patients with acute liver failure is correlated with arterial ammonia concentration. *Hepatology* 29, 648–653. doi: 10.1002/hep.510290309

Colon, A. D., Plaitakis, A., Perakis, A., Berl, S., and Clarke, D. D. (1986). Purification and characterization of a soluble and a particulate glutamate dehydrogenase from rat brain. *J. Neurochem.* 46, 1811–1819. doi: 10.1111/j.1471-4159.1986.tb08500.x

Cooper, A. J., Mora, S. N., Cruz, N. F., and Gelbard, A. S. (1985). Cerebral ammonia metabolism in hyperammonemic rats. *J. Neurochem.* 44, 1716–1723. doi: 10.1111/j.1471-4159.1985.tb07159.x

Craig, D. G., Lee, A., Hayes, P. C., and Simpson, K. J. (2010). Review article: the current management of acute liver failure. *Aliment. Pharmacol. Ther.* 31, 345–358. doi: 10.1111/j.1365-2036.2009.04175.x

Crompton, M., Costi, A., and Hayat, L. (1987). Evidence for the presence of a reversible $Ca^{2+}$-dependent pore activated by oxidative stress in heart mitochondria. *Biochem. J.* 245, 915–918. doi: 10.1042/bj2450915

Dabrowska, K., Skowronska, K., Popek, M., Obara-Michlewska, M., Albrecht, J., and Zielinska, M. (2018). Roles of glutamate and glutamine transport in ammonia neurotoxicity: state of the art and question marks. *Endocr. Metab. Immune Disord. Drug Targets* 18, 306–315. doi: 10.2174/1871520618666171219124427

Dam, G., Keiding, S., Munk, O. L., Ott, P., Vilstrup, H., Bak, L. K., et al. (2013). Hepatic encephalopathy is associated with decreased cerebral oxygen metabolism and blood flow, not increased ammonia uptake. *Hepatology* 57, 258–265. doi: 10.1002/hep.25995

de Assis, A. M., Rieger, D. K., Longoni, A., Battu, C., Raymundi, S., da Rocha, R. F., et al. (2009). High fat and highly thermolyzed fat diets promote insulin resistance and increase DNA damage in rats. *Exp. Biol. Med.* 234, 1296–1304. doi: 10.3181/0904-rm-126

Detry, O., Gaspar, Y., Cheramy-Bien, J. P., Drion, P., Meurisse, M., and Defraigne, J. O. (2013). A modified surgical model of fulminant hepatic failure in the rat. *J. Surg. Res.* 181, 85–90. doi: 10.1016/j.jss.2012.05.080

Dhanda, S., Sunkaria, A., Halder, A., and Sandhir, R. (2018). Mitochondrial dysfunctions contribute to energy deficits in rodent model of hepatic encephalopathy. *Metab. Brain Dis.* 33, 209–223. doi: 10.1007/s11011-017-0136-8

Dönmez, M., Uysal, B., Poyrazoğlu, Y., Öztas, Y. E., Türker, T., Kaldirim, Ü., et al. (2015). PARP inhibition prevents acetaminophen-induced liver injury and increases survival rate in rats. *Turk. J. Med. Sci.* 45, 18–26. doi: 10.3906/sag-1308-48

Dunlop, D. S., van Elden, W., and Lajtha, A. (1975). Optimal conditions for protein synthesis in incubated slices of rat brain. *Brain Res.* 99, 303–318. doi: 10.1016/0006-8993(75)90031-1

Eguchi, S., Kamlot, A., Ljubimova, J., Hewitt, W. R., Lebow, L. T., Demetriou, A. A., et al. (1996). Fulminant hepatic failure in rats: survival and effect on blood chemistry and liver regeneration. *Hepatology* 24, 1452–1459. doi: 10.1002/hep.510240626

El Khiat, A., Tamegart, L., Draoui, A., El Fari, R., Sellami, S., Rais, H., et al. (2019). Kinetic deterioration of short memory in rat with acute hepatic encephalopathy: involvement of astroglial and neuronal dysfunctions. *Behav. Brain Res.* 367, 201–209. doi: 10.1016/j.bbr.2019.03.046

Eustermann, S., Videler, H., Yang, J. C., Cole, P. T., Gruszka, D., Veprintsev, D., et al. (2011). The DNA-binding domain of human PARP-1 interacts with DNA single-strand breaks as a monomer through its second zinc finger. *J. Mol. Biol.* 407, 149–170. doi: 10.1016/j.jmb.2011.01.034

Ferreira, G. C., Tonin, A., Schuck, P. F., Viegas, C. M., Ceolato, P. C., Latini, A., et al. (2007). Evidence for a synergistic action of glutaric and 3-hydroxyglutaric acids disturbing rat brain energy metabolism. *Int. J. Dev. Neurosci.* 25, 391–398. doi: 10.1016/j.ijdevneu.2007.05.009

Fischer, J. C., Ruitenbeek, W., Berden, J. A., Trijbels, J. M., Veerkamp, J. H., Stadhouders, A. M., et al. (1985). Differential investigation of the capacity of succinate oxidation in human skeletal muscle. *Clin. Chim. Acta* 153, 23–36. doi: 10.1016/0009-8981(85)90135-4

Fitzpatrick, S. M., Hetherington, H. P., Behar, K. L., and Shulman, R. G. (1989). Effects of acute hyperammonemia on cerebral amino acid metabolism and pHi *in vivo*, measured by 1H and 31P nuclear magnetic resonance. *J. Neurochem.* 52, 741–749. doi: 10.1111/j.1471-4159.1989.tb02517.x

Fusco, S., Reitano, F., Gambadoro, N., Previti, M., Russo, G., Basile, G., et al. (2013). Severe hypoglycemia associated with levofloxacin in a healthy older woman. *J. Am. Geriatr. Soc.* 61, 1637–1638. doi: 10.1111/jgs.12436

Görg, B., Schliess, F., and Häussinger, D. (2013). Osmotic and oxidative/nitrosative stress in ammonia toxicity and hepatic encephalopathy. *Arch. Biochem. Biophys.* 536, 158–163. doi: 10.1016/j.abb.2013.03.010

Guo, C., Sun, L., Chen, X., and Zhang, D. (2013). Oxidative stress, mitochondrial damage and neurodegenerative diseases. *Neural Regen. Res.* 8, 2003–2014. doi: 10.3969/j.issn.1673-5374.2013.21.009

Hadjihambi, A., Arias, N., Sheikh, M., and Jalan, R. (2018). Hepatic encephalopathy: a critical current review. *Hepatol. Int.* 12, 135–147. doi: 10.1007/s12072-017-9812-3

Heidari, R. (2019). Brain mitochondria as potential therapeutic targets for managing hepatic encephalopathy. *Life Sci.* 218, 65–80. doi: 10.1016/j.lfs.2018.12.030

Hermenegildo, C., Monfort, P., and Felipo, V. (2000). Activation of N-methyl-D-aspartate receptors in rat brain *in vivo* following acute ammonia intoxication: characterization by *in vivo* brain microdialysis. *Hepatology* 31, 709–715. doi: 10.1002/hep.510310322

Hindfelt, B., Plum, F., and Duffy, T. E. (1977). Effect of acute ammonia intoxication on cerebral metabolism in rats with portacaval shunts. *J. Clin. Invest.* 59, 386–396. doi: 10.1172/jci108651

Hindfelt, B., and Siesjö, B. K. (1971). Cerebral effects of acute ammonia intoxication. II. The effect upon energy metabolism. *Scand. J. Clin. Lab. Invest.* 28, 365–374. doi: 10.3109/00365517109095711

Holmin, T., Agardh, C. D., Alinder, G., Herlin, P., and Hultberg, B. (1983). The influence of total hepatectomy on cerebral energy state, ammonia-related amino acids of the brain and plasma amino acids in the rat. *Eur. J. Clin. Invest.* 13, 215–220. doi: 10.1111/j.1365-2362.1983.tb00090.x

Iversen, P., Sorensen, M., Bak, L. K., Waagepetersen, H. S., Vafaee, M. S., Borghammer, P., et al. (2009). Low cerebral oxygen consumption and blood flow in patients with cirrhosis and an acute episode of hepatic encephalopathy. *Gastroenterology* 136, 863–871. doi: 10.1053/j.gastro.2008.10.057

Jayakumar, A. R., Rao, K. V., Murthy Ch, R., and Norenberg, M. D. (2006). Glutamine in the mechanism of ammonia-induced astrocyte swelling. *Neurochem. Int.* 48, 623–628. doi: 10.1016/j.neuint.2005.11.017

Johansen, M. L., Bak, L. K., Schousboe, A., Iversen, P., Sorensen, M., Keiding, S., et al. (2007). The metabolic role of isoleucine in detoxification of ammonia in cultured mouse neurons and astrocytes. *Neurochem. Int.* 50, 1042–1051. doi: 10.1016/j.neuint.2007.01.009

Jubin, T., Kadam, A., Jariwala, M., Bhatt, S., Sutariya, S., Gani, A. R., et al. (2016). The PARP family: insights into functional aspects of poly (ADP-ribose) polymerase-1 in cell growth and survival. *Cell Prolif.* 49, 421–437. doi: 10.1111/cpr.12268

Kaplan, J. L., Marshall, M. A., C, C. M., Harmon, D. B., Garmey, J. C., Oldham, S. N., et al. (2015). Adipocyte progenitor cells initiate monocyte chemoattractant protein-1-mediated macrophage accumulation in visceral adipose tissue. *Mol. Metab.* 4, 779–794. doi: 10.1016/j.molmet.2015.07.010

Keiding, S., and Pavese, N. (2013). Brain metabolism in patients with hepatic encephalopathy studied by PET and MR. *Arch. Biochem. Biophys.* 536, 131–142. doi: 10.1016/j.abb.2013.05.006

Kieling, C. O., Backes, A. N., Maurer, R. L., Cruz, C. U., Osvaldt, A. B., Silveira, T. R., et al. (2012). The effects of anesthetic regimen in 90% hepatectomy in rats. *Acta Cir. Bras.* 27, 702–706. doi: 10.1590/s0102-86502012001000006

Kimura, N., Kumamoto, T., Hanaoka, T., Nakamura, K., Hazama, Y., and Arakawa, R. (2008). Portal-systemic shunt encephalopathy presenting with diffuse cerebral white matter lesion: an autopsy case. *Neuropathology* 28, 627–632. doi: 10.1111/j.1440-1789.2008.00898.x

Kitto, G. B., Stolzenbach, F. E., and Kaplan, N. O. (1970). Mitochondrial malate dehydrogenase: further studies on multiple electrophoretic forms.

*Biochem. Biophys. Res. Commun.* 38, 31–39. doi: 10.1016/0006-291x(70)91079-x

Kosenko, E., Kaminsky, Y., Grau, E., Minana, M. D., Marcaida, G., Grisolia, S., et al. (1994). Brain ATP depletion induced by acute ammonia intoxication in rats is mediated by activation of the NMDA receptor and $Na^+$, $K^+$-ATPase. *J. Neurochem.* 63, 2172–2178. doi: 10.1046/j.1471-4159.1994.63062172.x

Kosenko, E., Kaminsky, Y., Kaminsky, A., Valencia, M., Lee, L., Hermenegildo, C., et al. (1997). Superoxide production and antioxidant enzymes in ammonia intoxication in rats. *Free Radic. Res.* 27, 637–644. doi: 10.3109/10715769709097867

Kosenko, E., Kaminsky, Y., Lopata, O., Muravyov, N., Kaminsky, A., Hermenegildo, C., et al. (1998). Nitroarginine, an inhibitor of nitric oxide synthase, prevents changes in superoxide radical and antioxidant enzymes induced by ammonia intoxication. *Metab. Brain Dis.* 13, 29–41. doi: 10.1023/a:1020626928259

Lai, J. C., and Cooper, A. J. (1986). Brain $\alpha$-ketoglutarate dehydrogenase complex: kinetic properties, regional distribution, and effects of inhibitors. *J. Neurochem.* 47, 1376–1386. doi: 10.1111/j.1471-4159.1986.tb00768.x

Langelier, M. F., Planck, J. L., Roy, S., and Pascal, J. M. (2011). Crystal structures of poly(ADP-ribose) polymerase-1 (PARP-1) zinc fingers bound to DNA: structural and functional insights into DNA-dependent PARP-1 activity. *J. Biol. Chem.* 286, 10690–10701. doi: 10.1074/jbc.M110.202507

Larsen, F. S., and Wendon, J. (2008). Prevention and management of brain edema in patients with acute liver failure. *Liver Transpl.* 14, S90–S96. doi: 10.1002/lt.21643

LeBel, C. P., Ischiropoulos, H., and Bondy, S. C. (1992). Evaluation of the probe 2′,7′-dichlorofluorescin as an indicator of reactive oxygen species formation and oxidative stress. *Chem. Res. Toxicol.* 5, 227–231. doi: 10.1021/tx00026a012

Lin, S., and Raabe, W. (1985). Ammonia intoxication: effects on cerebral cortex and spinal cord. *J. Neurochem.* 44, 1252–1258. doi: 10.1111/j.1471-4159.1985.tb08751.x

Madrahimov, N., Dirsch, O., Broelsch, C., and Dahmen, U. (2006). Marginal hepatectomy in the rat: from anatomy to surgery. *Ann. Surg.* 244, 89–98. doi: 10.1097/01.sla.0000218093.12408.0f

Mans, A. M., DeJoseph, M. R., and Hawkins, R. A. (1994). Metabolic abnormalities and grade of encephalopathy in acute hepatic failure. *J. Neurochem.* 63, 1829–1838. doi: 10.1046/j.1471-4159.1994.63051829.x

Martinez-Hernandez, A., Bell, K. P., and Norenberg, M. D. (1977). Glutamine synthetase: glial localization in brain. *Science* 195, 1356–1358. doi: 10.1126/science.14400

McPhail, M. J., Bajaj, J. S., Thomas, H. C., and Taylor-Robinson, S. D. (2010). Pathogenesis and diagnosis of hepatic encephalopathy. *Expert Rev. Gastroenterol. Hepatol.* 4, 365–378. doi: 10.1586/egh.10.32

Mirandola, S. R., Melo, D. R., Schuck, P. F., Ferreira, G. C., Wajner, M., and Castilho, R. F. (2008). Methylmalonate inhibits succinate-supported oxygen consumption by interfering with mitochondrial succinate uptake. *J. Inherit. Metab. Dis.* 31, 44–54. doi: 10.1007/s10545-007-0798-1

Montana, V., Verkhratsky, A., and Parpura, V. (2014). Pathological role for exocytotic glutamate release from astrocytes in hepatic encephalopathy. *Curr. Neuropharmacol.* 12, 324–333. doi: 10.2174/1570159x12666140903094700

Montes-Cortes, D. H., Olivares-Corichi, I. M., Rosas-Barrientos, J. V., Manuel-Apolinar, L., Martinez-Godinez, M. L. A., Hernandez-Lopez, J. C., et al. (2019). Characterization of oxidative stress and ammonia according to the different grades of hepatic encephalopathy. *Dig. Dis.* doi: 10.1159/000503097 [Epub ahead of print].

Müller, A. P., Longoni, A., Farina, M., da Silveira, C. K., Souza, D. O., Perry, M. L., et al. (2013). Propylthiouracil-induced hypothyroidism during lactation alters leucine and mannose metabolism in rat cerebellar slices. *Exp. Biol. Med.* 238, 31–36. doi: 10.1258/ebm.2012.012255

Murthy, C. R., Rama Rao, K. V., Bai, G., and Norenberg, M. D. (2001). Ammonia-induced production of free radicals in primary cultures of rat astrocytes. *J. Neurosci. Res.* 66, 282–288. doi: 10.1002/jnr.1222

Narciso, L., Parlanti, E., Racaniello, M., Simonelli, V., Cardinale, A., Merlo, D., et al. (2016). The response to oxidative DNA damage in neurons: mechanisms and disease. *Neural Plast.* 2016:3619274. doi: 10.1155/2016/3619274

Norenberg, M. D. (1996). Astrocytic-ammonia interactions in hepatic encephalopathy. *Semin. Liver Dis.* 16, 245–253. doi: 10.1055/-2007-1007237

Oja, S. S., Saransaari, P., and Korpi, E. R. (2017). Neurotoxicity of Ammonia. *Neurochem. Res.* 42, 713–720. doi: 10.1007/s11064-016-2014-x

Paniz, L. G., Calcagnotto, M. E., Pandolfo, P., Machado, D. G., Santos, G. F., Hansel, G., et al. (2014). Neuroprotective effects of guanosine administration on behavioral, brain activity, neurochemical and redox parameters in a rat model of chronic hepatic encephalopathy. *Metab. Brain Dis.* 29, 645–654. doi: 10.1007/s11011-014-9548-x

Pilbeam, C. M., Anderson, R. M., and Bhathal, P. S. (1983). The brain in experimental portal-systemic encephalopathy. I. Morphological changes in three animal models. *J. Pathol.* 140, 331–345. doi: 10.1002/path.1711400403

Rajaram, P., and Subramanian, R. (2018). Management of acute liver failure in the intensive care unit setting. *Clin. Liver Dis.* 22, 403–408. doi: 10.1016/j.cld.2018.01.013

Rama Rao, K. V., Jayakumar, A. R., and Norenberg, M. D. (2014). Brain edema in acute liver failure: mechanisms and concepts. *Metab. Brain Dis.* 29, 927–936. doi: 10.1007/s11011-014-9502-y

Rosenthal, R. E., Hamud, F., Fiskum, G., Varghese, P. J., and Sharpe, S. (1987). Cerebral ischemia and reperfusion: prevention of brain mitochondrial injury by lidoflazine. *J. Cereb. Blood Flow Metab.* 7, 752–758. doi: 10.1038/jcbfm.1987.130

Sathyasaikumar, K. V., Swapna, I., Reddy, P. V., Murthy Ch, R., Dutta Gupta, A., Senthilkumaran, B., et al. (2007). Fulminant hepatic failure in rats induces oxidative stress differentially in cerebral cortex, cerebellum and pons medulla. *Neurochem. Res.* 32, 517–524. doi: 10.1007/s11064-006-9265-x

Schousboe, A., Waagepetersen, H. S., Leke, R., and Bak, L. K. (2014). Effects of hyperammonemia on brain energy metabolism: controversial findings *in vivo* and *in vitro*. *Metab. Brain Dis.* 29, 913–917. doi: 10.1007/s11011-014-9513-8

Scott, T. R., Kronsten, V. T., Hughes, R. D., and Shawcross, D. L. (2013). Pathophysiology of cerebral oedema in acute liver failure. *World J. Gastroenterol.* 19, 9240–9255. doi: 10.3748/wjg.v19.i48.9240

Shepherd, D., and Garland, P. B. (1969). The kinetic properties of citrate synthase from rat liver mitochondria. *Biochem. J.* 114, 597–610. doi: 10.1042/bj1140597

Sibson, N. R., Mason, G. F., Shen, J., Cline, G. W., Herskovits, A. Z., Wall, J. E., et al. (2001). *In vivo* (13)C NMR measurement of neurotransmitter glutamate cycling, anaplerosis and TCA cycle flux in rat brain during. *J. Neurochem.* 76, 975–989. doi: 10.1046/j.1471-4159.2001.00074.x

Souza, D. G., Almeida, R. F., Souza, D. O., and Zimmer, E. R. (2019). The astrocyte biochemistry. *Semin. Cell Dev. Biol.* 95, 142–150. doi: 10.1016/j.semcdb.2019.04.002

Strauss, G. I., Møller, K., Larsen, F. S., Kondrup, J., and Knudsen, G. M. (2003). Cerebral glucose and oxygen metabolism in patients with fulminant hepatic failure. *Liver Transpl.* 9, 1244–1252. doi: 10.1016/j.lts.2003.09.020

Stravitz, R. T., and Larsen, F. S. (2009). Therapeutic hypothermia for acute liver failure. *Crit. Care Med.* 37, S258–S264. doi: 10.1097/CCM.0b013e3181aa5fb8

Tretter, L., and Adam-Vizi, V. (2004). Generation of reactive oxygen species in the reaction catalyzed by $\alpha$-ketoglutarate dehydrogenase. *J. Neurosci.* 24, 7771–7778. doi: 10.1523/JNEUROSCI.1842-04.2004

Ulm, J. W., Perron, M., Sodroski, J., and R, C. M. (2007). Complex determinants within the Moloney murine leukemia virus capsid modulate susceptibility of the virus to Fv1 and Ref1-mediated restriction. *Virology* 363, 245–255. doi: 10.1016/j.virol.2006.09.048

Voelter, W., Zech, K., Arnold, P., and Ludwig, G. (1980). Determination of selected pyrimidines, purines and their metabolites in serum and urine by reversed-phase ion-pair chromatography. *J. Chromatogr.* 199, 345–354. doi: 10.1016/s0021-9673(01)91386-x

Walker, V. (2014). Ammonia metabolism and hyperammonemic disorders. *Adv. Clin. Chem.* 67, 73–150. doi: 10.1016/bs.acc.2014.09.002

Warskulat, U., Görg, B., Bidmon, H. J., Müller, H. W., Schliess, F., and Häussinger, D. (2002). Ammonia-induced heme oxygenase-1 expression in cultured rat astrocytes and rat brain *in vivo*. *Glia* 40, 324–336. doi: 10.1002/glia.10128

Wendel, A. (1981). Glutathione peroxidase. *Meth. Enzymol.* 77, 325–333. doi: 10.1016/s0076-6879(81)77046-0

Xue, Z., Li, B., Gu, L., Hu, X., Li, M., Butterworth, R. F., et al. (2010). Increased Na, K-ATPase $\alpha 2$ isoform gene expression by ammonia in astrocytes and in brain *in vivo*. *Neurochem. Int.* 57, 395–403. doi: 10.1016/j.neuint.2010.04.014

Zoratti, M., Szabò, I., and De Marchi, U. (2005). Mitochondrial permeability transitions: how many doors to the house? *Biochim. Biophys. Acta* 1706, 40–52. doi: 10.1016/j.bbabio.2004.10.006

Zwingmann, C., Chatauret, N., Leibfritz, D., and Butterworth, R. F. (2003). Selective increase of brain lactate synthesis in experimental acute liver failure: results of a [H-C] nuclear magnetic resonance study. *Hepatology* 37, 420–428. doi: 10.1053/jhep.2003.50052

**Conflict of Interest**: The authors declare that the research was conducted in the absence of any commercial or financial relationships that could be construed as a potential conflict of interest.